Momentum distribution of the insulating phases of the extended Bose-Hubbard model

M. Iskin[1] and J. K. Freericks[2]
[1]*Joint Quantum Institute, National Institute of Standards and Technology and University of Maryland, Gaithersburg, Maryland 20899-8423, USA*
[2]*Department of Physics, Georgetown University, Washington, DC 20057, USA*
(Received 7 May 2009; revised manuscript received 2 October 2009; published 4 December 2009)

We develop two methods to calculate the momentum distribution of the insulating (Mott and charge-density-wave) phases of the extended Bose-Hubbard model with on-site and nearest-neighbor boson-boson repulsions on d-dimensional hypercubic lattices. First, we construct the random-phase approximation result, which corresponds to the exact solution for the infinite-dimensional limit. Then, we perform a power-series expansion in the hopping t via strong-coupling perturbation theory, to evaluate the momentum distribution in two and three dimensions; we also use the strong-coupling theory to verify the random-phase approximation solution in infinite dimensions. Finally, we briefly discuss possible implications of our results in the context of ultracold dipolar Bose gases with dipole-dipole interactions loaded into optical lattices.

DOI: 10.1103/PhysRevA.80.063610 PACS number(s): 03.75.Lm, 37.10.Jk, 67.85.−d

I. INTRODUCTION

Ultracold atomic gases loaded into optical lattices have been proven to be ideal systems for studying Hubbard-type Hamiltonians [1], the most successful of which has been the Bose-Hubbard (BH) model. This model has three terms [2]: a kinetic energy term which allows for the tunneling of the bosons between nearest-neighbor lattice sites, a potential energy term that is given by the repulsion between bosons that occupy the same lattice site, and a chemical potential term that fixes the number of bosons. The phase diagram of this model has been known for a long time [2–7]. The competition between the kinetic and potential energy terms leads to two phases: a Mott insulator (Mott) when the kinetic energy is much smaller than the potential energy and a superfluid otherwise. The Mott phase has an excitation gap and is incompressible, and therefore, the bosons are localized and incoherent, so that a slight change in the chemical potential does not change the number of bosons on a particular lattice site. The superfluid phase, however, is gapless and compressible, and the bosons are delocalized and move coherently. Both of these phases, as well as the transition between the two, have been successfully observed with ultracold pointlike Bose gases loaded into optical lattices [8–11].

The on-site BH model takes only the on-site boson-boson repulsion into account, i.e., the interaction is short-ranged. A more general extended BH model is required when longer-ranged interactions are not negligible, e.g., Coulomb or dipole-dipole interactions. For instance, an ultracold dipolar Bose gas can be realized in many ways with optical lattices [12]: (ground-state) heteronuclear molecules that have permanent electric dipole moments, Rydberg atoms that have very large induced electric dipole moment, or Chromium-like atoms that have large intrinsic magnetic moment, etc. can be used to generate sufficiently strong long-ranged dipole-dipole interactions. The qualitative phase diagram of this model has also been known for a long time [13–19], and it has two additional phases: a charge-density wave (CDW) as shown in Fig. 1 and a supersolid. Similar to the Mott phase, the CDW phase is an insulator with an excitation gap and it is incompressible. The main difference is that an integer number of bosons occupy every lattice site in the Mott phase, while the CDW phase has a crystalline order in the form of staggered boson numbers (different occupancy on different sublattices). As the name suggests, a supersolid phase [20], however, has both the superfluid and crystalline orders, i.e., both CDW and superfluid phases coexist. There is some evidence that this phase exists only in dimensions higher than one [15,16].

There has been experimental progress in constructing ultracold dipolar gases of molecules, namely, ground-state K-Rb molecules, from a mixture of fermionic ^{40}K and bosonic ^{87}Rb atoms [21,22]. While this K-Rb is a fermionic molecule, similar principles will allow one to also create bosonic dipolar molecules by simply changing the atomic isotopes. Motivated by these achievements, in this paper, we analyze the momentum distribution of the insulating phases of the extended BH model, which is the most common probing technique used in atomic systems to identify different phases.

The remainder of this paper is organized as follows. After presenting the model Hamiltonian in Sec. II, we develop two methods in Sec. III to calculate the momentum distribution of the insulating (Mott or charge-density-wave) phases of the extended Bose-Hubbard model. First, we use the random-phase approximation (RPA) in Sec. III A, and then we perform a power-series expansion in the hopping t via the strong-coupling perturbation theory in Sec. III B. The numerical analysis of the momentum distribution obtained from these methods is discussed in Sec. III C, and a brief summary of our conclusions is presented in Sec. IV.

II. EXTENDED BOSE-HUBBARD MODEL

We consider the following extended BH Hamiltonian with on-site and nearest-neighbor boson-boson repulsions

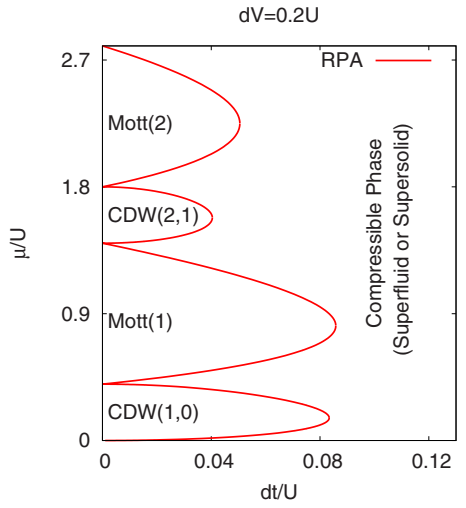

FIG. 1. (Color online) We show the chemical potential μ (in units of U) versus hopping t (in units of U/d) phase diagram within the random-phase approximation for d-dimensional hypercubic lattices (it becomes exact for $d\to\infty$). Here, the nearest-neighbor repulsion scales inversely with d such that $dV=0.2U$. The red solid line corresponds to phase boundaries for the Mott insulator to superfluid and CDW insulator to supersolid states as obtained from Eq. (5).

$$H = -\sum_{i,j} t_{ij} b_i^\dagger b_j + \frac{U}{2}\sum_i \hat{n}_i(\hat{n}_i - 1) + \sum_{i,j} V_{ij}\hat{n}_i\hat{n}_j - \mu\sum_i \hat{n}_i, \tag{1}$$

where t_{ij} is the tunneling (or hopping) matrix between sites i and j, $b_i^\dagger(b_i)$ is the boson creation (annihilation) operator at site i, $\hat{n}_i=b_i^\dagger b_i$ is the boson number operator, $U>0$ is the strength of the on-site and V_{ij} is the longer-ranged boson-boson repulsion between bosons at sites i and j, and μ is the chemical potential. In this paper, we assume t_{ij} is a real symmetric matrix with elements $t_{ij}=t$ for i and j nearest neighbors and 0 otherwise and similarly for V_{ij} (equal to $V>0$ for i and j nearest neighbors and zero otherwise), and consider a d-dimensional hypercubic lattice with M sites. Note that we work on a periodic lattice without an external trapping potential. We also assume $U>zV$ where $z=2d$ is the lattice coordination number (number of nearest neighbors).

The ground-state phase diagram of this model Hamiltonian has been studied extensively in the literature including the mean-field [13], quantum Monte Carlo [14,15], density-matrix renormalization group [16], Gutzwiller ansatz [17,18], and strong-coupling expansion and scaling theory [19] techniques. When $V\neq 0$, the ground state now has two types of insulating phases. The first one is the Mott phase where, similar to the on-site BH model, the ground-state boson occupancy is the same for every lattice site, i.e., $\langle\hat{n}_i\rangle=n_0$. Here, $\langle\ldots\rangle$ is the thermal average, and the average boson occupancy n_0 is chosen to minimize the ground-state energy for a given μ. The second one is the CDW phase, which has crystalline order in the form of staggered boson occupancies, i.e., $\langle\hat{n}_i\rangle=n_A$ and $\langle\hat{n}_j\rangle=n_B$ for i and j nearest neighbors. To describe the CDW, it is convenient to split the entire lattice into two sublattices A and B such that the nearest-neighbor sites belong to a different sublattice. A lattice for which this can be done is called a bipartite lattice, and we assume the number of lattice sites in each sublattice is the same $(M/2)$. We also assume that the boson occupancies of the sublattices A and B are n_A and n_B, respectively, such that $n_A\geq n_B$. The case with $n_A=n_B=n_0$ corresponds to the Mott phase.

When $t=0$, it turns out that the chemical potential width of all Mott and CDW lobes are U and zV, respectively, and that the ground state alternates between the CDW and Mott phases as a function of increasing μ [13–19]. For instance, the ground state is a vacuum $(n_A=0,\ n_B=0)$ for $\mu\leq 0$; it is a CDW with $(n_A=1,\ n_B=0)$ for $0\leq\mu\leq zV$; it is a Mott insulator with $(n_A=1,\ n_B=1)$ for $zV\leq\mu\leq U+zV$; it is a CDW with $(n_A=2,\ n_B=1)$ for $U+zV\leq\mu\leq U+2zV$; it is a Mott insulator with $(n_A=2,\ n_B=2)$ for $U+2zV\leq\mu\leq 2U+2zV$, and so on. As t increases, the range of μ about which the ground state is insulating decreases, and the Mott and CDW phases disappear at a critical value of t, beyond which the system becomes compressible (superfluid or supersolid) as shown in Fig. 1.

Identification of these phases in atomic systems loaded into optical lattices is a real challenge, and the momentum distribution of particles has been the most commonly used probing technique to distinguish superfluid and Mott phases of the on-site BH model. Motivated by these experiments, next, we analyze the momentum distribution of the insulating phases of the extended BH model, paying particular attention to what signatures one might see that can distinguish the CDW insulating phase.

III. MOMENTUM DISTRIBUTION

The momentum distribution of the atoms is one of the few (and probably the easiest) physical quantity that can be directly probed in experiments with ultracold atomic gases. This is achieved by time-of-flight absorption imaging of freely expanding atoms that are released from the trap. Since ultracold gases are very dilute, atoms do not interact much with each other during this short time-of-flight, and therefore, the particle positions in the absorption image are strongly correlated with their velocity distribution given by their momentum distribution at the moment of release from the trap.

The momentum distribution $n(\mathbf{k})$ is also easy to calculate, and it is defined as the Fourier transform of the one-particle density-matrix $\rho(\mathbf{r},\mathbf{r}')=\langle\psi^\dagger(\mathbf{r})\psi(\mathbf{r}')\rangle$, such that $n(\mathbf{k})=\int d\mathbf{r}\int d\mathbf{r}'\rho(\mathbf{r},\mathbf{r}')e^{i\mathbf{k}\cdot(\mathbf{r}-\mathbf{r}')}$, where $\psi^\dagger(\mathbf{r})[\psi(\mathbf{r})]$ is the boson creation (annihilation) field operator, and $\mathbf{k}$ is the momentum. We expand the field operators in the basis set of Wannier functions such that $\psi(\mathbf{r})=(1/\sqrt{M})\Sigma_\ell W(\mathbf{r}-\mathbf{R}_\ell)b_\ell$, where M is the number of lattice sites, and the Wannier function $W(\mathbf{r}-\mathbf{R}_\ell)$ is localized at site ℓ with position $\mathbf{R}_\ell$. Here, the summation index $\ell\in\{A,B\}$ includes the entire lattice.

In this paper, we use two methods to calculate the momentum distribution of the insulating phases of the extended BH model. First, we calculate $n(\mathbf{k})$ via the RPA theory in Sec. III A, and its result corresponds to the exact result for

the infinite-dimensional limit. Then, in Sec. III B, we calculate $n(\mathbf{k})$ as a power-series expansion in the hopping t via the strong-coupling perturbation theory. We also verify that our strong-coupling expansion recovers the RPA result in the infinite-dimensional limit when the latter is expanded out in t to the same order. This provides an independent cross-check of the algebra as discussed next in detail.

A. Random-Phase Approximation (RPA)

Using the standard-basis operator method developed by Haley and Erdös [23], and following the recent works on the on-site BH model [24–28], here we obtain the equation of motion for the insulating phases of the extended BH model. This approximation is a well-defined linear operation in which thermal averages of products of operators are replaced by the product of their thermal averages. In accordance with this approximation, the three-operator Green's functions are reduced to two-operator ones [23]. Therefore, the RPA method allows us to calculate the single-particle Green's function $G(\mathbf{k},i\omega_n)=-\langle\psi(\mathbf{k},i\omega_n)\psi^{\dagger}(\mathbf{k},i\omega_n)\rangle$ in momentum ($\mathbf{k}$) and Matsubara frequency ($i\omega_n$) space, from which the spectral function $A(\mathbf{k},\omega)=-(1/\pi)\mathrm{Im}\, G(\mathbf{k},i\omega_n\rightarrow\omega+i\epsilon)$ can be extracted by analytical continuation. Here, the angular brackets denote the standard trace over the density matrix. Notice that the spectral function should always satisfy the sum rule $\int_{-\infty}^{\infty}A(\mathbf{k},\omega)d\omega=1$, due to the bosonic commutation relations of the creation and annihilation operators in the Heisenberg picture at equal times. Then, the momentum distribution $n(\mathbf{k})=\langle\psi^{\dagger}(\mathbf{k})\psi(\mathbf{k})\rangle$ (at zero temperature) can be easily obtained from the spectral function $n(\mathbf{k})=-\int_{-\infty}^{0}A(\mathbf{k},\omega)d\omega$, i.e.,

$$n(\mathbf{k})=\frac{1}{\pi}\int_{-\infty}^{0}\mathrm{Im}\, G(\mathbf{k},i\omega_n\rightarrow\omega+i\epsilon)d\omega, \tag{2}$$

which measures the spectral weight of the hole excitation spectrum.

Expanding the field operators in the basis set of Wannier functions, the momentum distribution becomes

$$n(\mathbf{k})=\frac{|W(\mathbf{k})|^2}{M}\sum_{\ell,\ell'}\langle b_{\ell}^{\dagger}b_{\ell'}\rangle e^{-i\mathbf{k}\cdot(\mathbf{R}_{\ell}-\mathbf{R}_{\ell'})}, \tag{3}$$

where $W(\mathbf{k})=\int d\mathbf{r}W(\mathbf{r})e^{i\mathbf{k}\cdot\mathbf{r}}$ is the Fourier transform of $W(\mathbf{r})$. Here, the summation indices $\ell\in\{A,B\}$ and $\ell'\in\{A,B\}$ include the entire lattice. Since $W(\mathbf{k})$ is a nonuniversal property of the lattice potential, and it has nothing to do with the extended BH model on a discrete periodic lattice, we ignore this function in this paper by setting it to unity.

But before beginning the discussion of our formal treatment of the theory, we want to comment further on the subtle features that arise for the momentum distribution $n(\mathbf{k})$ in an ordered phase, when the lattice periodicity is further broken by the spontaneous appearance of the CDW phase with a lower lattice periodicity. This system becomes that of a lattice with a basis, as the A and B sublattices now have a different occupancies of particles on them. When examining $n(\mathbf{k})$ on the lattice, we evaluate the one-particle density matrix at each lattice site $\rho(\mathbf{r},\mathbf{r}')\rightarrow\rho(\mathbf{R}_i,\mathbf{R}_j)=\rho_{ij}$. The integral in the definition of $n(\mathbf{k})$ is replaced by a summation *that extends over all lattice sites of the original lattice (before the CDW order occurred)*. We can break this summation up into terms that involve solely the A sublattice, solely the B sublattice, and terms that mix the A and B sublattices. One can immediately see that the terms restricted to one of the sublattices are periodic with the periodicity of the reduced Brillouin zone, while the mixed terms are only periodic with respect to the full Brillouin zone. If we assume the Wannier functions are identical for the A and B sublattices, then this uniform weighting of the different contributions yields the correct momentum distribution; in general, one potentially has different weightings of the three different components. A full discussion of this issue is beyond this work, where we focus on the properties of the pure discrete lattice system, not on the experimental systems which have the additional real-space structure arising from the spatial continuum.

The fluctuations are not fully taken into account in the RPA method, however, it goes beyond the mean-field approximation for low-dimensional systems, and it becomes exact for infinite-dimensional bosonic systems recovering the mean-field theory. The RPA method has recently been applied to describe the superfluid and Mott phases of the on-site BH model [25,26], and its results showed good agreement with the experiments. Motivated by these earlier works, here, we generalize this method to describe the insulating phases of the extended BH model.

Keeping in mind our two-sublattice system, the single-particle Green's function in momentum and frequency space can be written as $G(\mathbf{k},i\omega_n)=(1/2)\Sigma_{S,S'}G_{SS'}(\mathbf{k},i\omega_n)$, where the indices S and S' label sublattices $\{A,B\}$, and $G_{SS'}(\mathbf{k},i\omega_n)=(2/M)\Sigma_{\ell\in S,\ell'\in S'}G_{\ell\ell'}(i\omega_n)e^{-i\mathbf{k}\cdot(\mathbf{R}_{\ell}-\mathbf{R}_{\ell'})}$ is the Fourier transform. Here, the summation indices $\ell\in A$ or B and $\ell'\in A$ or B include only one sublattice and the Green's function is defined only at the different lattice positions. Since there are $M/2$ lattice sites in one sublattice, a factor of 2 appears in this expression. Note that this is just a rewriting of the summation over all lattice sites that explicitly shows the contributions from the different sublattices. The RPA equations have the following form in position and frequency space $G_{\ell\ell'}(i\omega_n)=G_{\ell}^{0}(i\omega_n)[\delta_{\ell\ell'}+\Sigma_{\ell''}J_{\ell\ell''}G_{\ell''\ell'}(i\omega_n)]$, where $G_{\ell}^{0}(i\omega_n)$ and $J_{\ell\ell''}$ are given below Eq. (4). Here, the indices ℓ, ℓ', and $\ell''\in\{A,B\}$ include the entire lattice. Using the Fourier transforms, the RPA equation in momentum and frequency space becomes $G_{SS'}(\mathbf{k},i\omega_n)=G_{S}^{0}(\mathbf{k},i\omega_n)[\delta_{SS'}+\Sigma_{S''}J_{SS''}(\mathbf{k})G_{S''S'}(\mathbf{k},i\omega_n)]$. This expression defines a set of coupled equations for the functions $G_{AA}(\mathbf{k},i\omega_n)$, $G_{AB}(\mathbf{k},i\omega_n)$, $G_{BA}(\mathbf{k},i\omega_n)$, and $G_{BB}(\mathbf{k},i\omega_n)$.

Since hopping is allowed between nearest-neighbor sites that belong to different sublattices, $J_{AA}(\mathbf{k})=J_{BB}(\mathbf{k})=0$ and $J_{AB}(\mathbf{k})=J_{BA}(\mathbf{k})=\varepsilon(\mathbf{k})$, where $\varepsilon(\mathbf{k})$ is the Fourier transform of the hopping matrix (also called the band structure). For d-dimensional hypercubic lattices considered in this paper, the energy dispersion becomes $\varepsilon(\mathbf{k})=-2t\Sigma_{i=1}^{d}\cos(k_ia)$, where a is the lattice spacing. This then yields the following expression for the Green's function

$$G_{\mathrm{Ins}}(\mathbf{k},i\omega_n)=\frac{G_{\mathrm{avr}}^{0}(i\omega_n)+\varepsilon(\mathbf{k})G_{A}^{0}(i\omega_n)G_{B}^{0}(i\omega_n)}{1-\varepsilon^2(\mathbf{k})G_{A}^{0}(i\omega_n)G_{B}^{0}(i\omega_n)}, \tag{4}$$

where $G_{\mathrm{avr}}^{0}(i\omega_n)=[G_{A}^{0}(i\omega_n)+G_{B}^{0}(i\omega_n)]/2$. The $\mathbf{k}$-independent functions $G_{A}^{0}(i\omega_n)$ and $G_{B}^{0}(i\omega_n)$ correspond to the single-

particle local Green's functions for sublattices A and B, respectively, at zeroth order in t. They have the familiar form $G_S^0(i\omega_n)=(n_S+1)/(i\omega_n-E_S^{\rm par})-n_S/(i\omega_n+E_S^{\rm hol})$, where $E_A^{\rm par}=Un_A+zVn_B-\mu$ and $E_B^{\rm par}=Un_B+zVn_A-\mu$ are the zeroth-order particle excitation spectrum in t (the energy required to add one extra particle) for sublattices A and B, respectively, and similarly $E_A^{\rm hol}=-U(n_A-1)-zVn_B+\mu$ and $E_B^{\rm hol}=-U(n_B-1)-zVn_A+\mu$ are the zeroth-order hole excitation spectrum in t (the energy required to remove one particle). Notice that $G_{\rm Ins}(\mathbf{k},i\omega_n)=G_{\rm avr}^0(i\omega_n)$ at zeroth order in t, as one may expect.

The poles of $G_{\rm Ins}(\mathbf{k},i\omega_n)$, i.e., the condition $1=\varepsilon^2(\mathbf{k})G_A^0(i\omega_n)G_B^0(i\omega_n)$, give the $\mathbf{k}$-dependence of the particle and hole excitation spectrum. The insulating phase becomes unstable against superfluidity when any of the excitation energies becomes negative at $\mathbf{k}=0$. In addition, the poles of $G_{\rm Ins}(\mathbf{k},i\omega_n)$ at $(\mathbf{k}=0,\ i\omega_n=0)$, i.e., the condition $1=\varepsilon^2(0)G_A^0(0)G_B^0(0)$, gives the mean-field phase boundary between the incompressible (Mott or CDW) and the compressible (superfluid or supersolid) phases. This condition leads to

$$\frac{1}{z^2t^2}=\left(\frac{n_A+1}{E_A^{\rm par}}+\frac{n_A}{E_A^{\rm hol}}\right)\left(\frac{n_B+1}{E_B^{\rm par}}+\frac{n_B}{E_B^{\rm hol}}\right), \tag{5}$$

which is a quartic equation for μ, and it coincides with our earlier result [19]. Notice that Eq. (5) reduces to the usual expression for the phase boundary of the on-site BH model when $n_A=n_B=n_0$ and $V=0$. Having discussed the general RPA formalism for the insulating phases of the extended BH model, next, we analyze the momentum distribution of the Mott and CDW phases separately.

1. Mott Phase

The single-particle Green's function for the Mott phase can be obtained from Eq. (4) by setting $n_A=n_B=n_0$. This leads to $G_{\rm Mott}(\mathbf{k},i\omega_n)=G_0^0(i\omega_n)/[1-\varepsilon(\mathbf{k})G_0^0(i\omega_n)]$, which has the same form with that of the Green's function of the Mott phase in the on-site BH model [25,26,28]. Here, $G_A^0(i\omega_n)=G_B^0(i\omega_n)=G_0^0(i\omega_n)$. The function $G_{\rm Mott}(\mathbf{k},i\omega_n)$ has two poles at $i\omega_n=E_0^{\rm par}(\mathbf{k})$ and $i\omega_n=-E_0^{\rm hol}(\mathbf{k})$, where, $E_0^{\rm par}(\mathbf{k})=E_0^{\rm par}-[U-\varepsilon(\mathbf{k})-E_0(\mathbf{k})]/2$ and $E_0^{\rm hol}(\mathbf{k})=E_0^{\rm hol}-[U+\varepsilon(\mathbf{k})-E_0(\mathbf{k})]/2$ corresponding to the particle (the energy required to add one extra particle) and hole (the energy required to remove one particle) excitation spectrum, respectively, where $E_0(\mathbf{k})=\sqrt{\varepsilon^2(\mathbf{k})+2U(2n_0+1)\varepsilon(\mathbf{k})+U^2}$. Notice that the Mott insulator becomes unstable against superfluidity when $E_0^{\rm par}(0)=0$ or $E_0^{\rm hol}(0)=0$, and these conditions coincide with the mean-field condition given in Eq. (5) when $n_A=n_B=n_0$.

Therefore, the Green's function for the Mott phase can be written as

$$G_{\rm Mott}(\mathbf{k},i\omega_n)=\frac{C_0^{\rm par}(\mathbf{k})}{i\omega_n-E_0^{\rm par}(\mathbf{k})}+\frac{C_0^{\rm hol}(\mathbf{k})}{i\omega_n+E_0^{\rm hol}(\mathbf{k})}, \tag{6}$$

where the coefficients (or the spectral weights) are functions of the excitation spectrum

$$C_0^{\rm par}(\mathbf{k})=\frac{E_0^{\rm par}(\mathbf{k})+Un_0+E_0^{\rm hol}}{E_0^{\rm par}(\mathbf{k})+E_0^{\rm hol}(\mathbf{k})}, \tag{7}$$

$$C_0^{\rm hol}(\mathbf{k})=\frac{E_0^{\rm hol}(\mathbf{k})-Un_0-E_0^{\rm hol}}{E_0^{\rm par}(\mathbf{k})+E_0^{\rm hol}(\mathbf{k})}. \tag{8}$$

Using the definition given above Eq. (2), the spectral function for the Mott phase can be easily obtained from Eq. (6), leading to $A_{\rm Mott}(\mathbf{k},\omega)=C_0^{\rm par}(\mathbf{k})\delta[\omega-E_0^{\rm par}(\mathbf{k})]+C_0^{\rm hol}(\mathbf{k})\delta[\omega+E_0^{\rm hol}(\mathbf{k})]$, where $\delta(x)$ is the Delta function defined by $\delta(x)=(1/\pi)\lim_{\epsilon\to0}\epsilon/(x^2+\epsilon^2)$. Notice that this function satisfies the sum rule mentioned above Eq. (2), since the coefficients satisfy $C_0^{\rm par}(\mathbf{k})+C_0^{\rm hol}(\mathbf{k})=1$. The momentum distribution measures the spectral weight of the hole excitation spectrum as defined in Eq. (2), and for the Mott phase it is given by

$$n_{\rm Mott}(\mathbf{k})=-C_0^{\rm hol}(\mathbf{k})=\frac{U(2n_0+1)+\varepsilon(\mathbf{k})}{2E_0(\mathbf{k})}-\frac{1}{2}, \tag{9}$$

which is identical to the $n_{\rm Mott}(\mathbf{k})$ of the on-site BH model [25,26]. Therefore, at the RPA level, $n_{\rm Mott}(\mathbf{k})$ is independent of V, which is mainly because of the underlying mean-field Hamiltonian that is used in the RPA formalism (we remind that fluctuations are not fully taken into account within RPA). For instance, the mean-field phase boundary condition given in Eq. (5) shows that the Mott lobes are separated by zV, but their shapes and, in particular, the critical points are independent of V. This point will become more clear in Sec. III B, where we analyze $n(\mathbf{k})$ via the strong-coupling perturbation theory up to second order in t. Notice that the momentum distribution is flat and equals the average filling fraction $n_{\rm Mott}(\mathbf{k})=n_0$ at zeroth order in t, corresponding to vanishing site-to-site correlations.

2. CDW Phase

In contrast to the Green's function of the Mott phase, the single-particle Green's function for the CDW phase $G_{\rm CDW}(\mathbf{k},i\omega_n)$ has four poles. Two of them correspond to the particle and the other two to the hole excitation spectrum of sublattices A and B. Unfortunately, general expressions for these poles are not analytically tractable since the condition $1=\varepsilon^2(\mathbf{k})G_A^0(i\omega_n)G_B^0(i\omega_n)$ defines a quartic equation for $i\omega_n$; they can be easily obtained numerically for any given CDW lobe as shown in Sec. III C. Assuming that the excitation spectrum is known, the Green's function for the CDW phase can be written as

$$G_{\rm CDW}(\mathbf{k},i\omega_n)=\frac{C_A^{\rm par}(\mathbf{k})}{i\omega_n-E_A^{\rm par}(\mathbf{k})}+\frac{C_A^{\rm hol}(\mathbf{k})}{i\omega_n+E_A^{\rm hol}(\mathbf{k})}+\frac{C_B^{\rm par}(\mathbf{k})}{i\omega_n-E_B^{\rm par}(\mathbf{k})}+\frac{C_B^{\rm hol}(\mathbf{k})}{i\omega_n+E_B^{\rm hol}(\mathbf{k})}, \tag{10}$$

where $E_A^{\rm par}(\mathbf{k})$ and $E_B^{\rm par}(\mathbf{k})$ are the particle (the energy required to add one extra particle) and $E_A^{\rm hol}(\mathbf{k})$ and $E_B^{\rm hol}(\mathbf{k})$ are the hole (the energy required to remove one particle) excitation spectrum. The coefficients (or the spectral weights) are functions of the excitation spectrum, such that

$$C_A^{\mathrm{par}}(\mathbf{k}) = \frac{D_0(\mathbf{k}) + D_1(\mathbf{k})E_A^{\mathrm{par}}(\mathbf{k}) + D_2(\mathbf{k})[E_A^{\mathrm{par}}(\mathbf{k})]^2 + [E_A^{\mathrm{par}}(\mathbf{k})]^3}{[E_A^{\mathrm{par}}(\mathbf{k}) - E_B^{\mathrm{par}}(\mathbf{k})][E_A^{\mathrm{par}}(\mathbf{k}) + E_B^{\mathrm{hol}}(\mathbf{k})][E_A^{\mathrm{par}}(\mathbf{k}) + E_A^{\mathrm{hol}}(\mathbf{k})]}, \tag{11}$$

$$C_B^{\mathrm{par}}(\mathbf{k}) = \frac{D_0(\mathbf{k}) + D_1(\mathbf{k})E_B^{\mathrm{par}}(\mathbf{k}) + D_2(\mathbf{k})[E_B^{\mathrm{par}}(\mathbf{k})]^2 + [E_B^{\mathrm{par}}(\mathbf{k})]^3}{[E_B^{\mathrm{par}}(\mathbf{k}) - E_A^{\mathrm{par}}(\mathbf{k})][E_B^{\mathrm{par}}(\mathbf{k}) + E_A^{\mathrm{hol}}(\mathbf{k})][E_B^{\mathrm{par}}(\mathbf{k}) + E_B^{\mathrm{hol}}(\mathbf{k})]}, \tag{12}$$

$$C_A^{\mathrm{hol}}(\mathbf{k}) = \frac{D_0(\mathbf{k}) - D_1(\mathbf{k})E_A^{\mathrm{hol}}(\mathbf{k}) + D_2(\mathbf{k})[E_A^{\mathrm{hol}}(\mathbf{k})]^2 - [E_A^{\mathrm{hol}}(\mathbf{k})]^3}{[E_B^{\mathrm{hol}}(\mathbf{k}) - E_A^{\mathrm{hol}}(\mathbf{k})][E_A^{\mathrm{hol}}(\mathbf{k}) + E_B^{\mathrm{par}}(\mathbf{k})][E_A^{\mathrm{hol}}(\mathbf{k}) + E_A^{\mathrm{par}}(\mathbf{k})]}, \tag{13}$$

$$C_B^{\mathrm{hol}}(\mathbf{k}) = \frac{D_0(\mathbf{k}) - D_1(\mathbf{k})E_B^{\mathrm{hol}}(\mathbf{k}) + D_2(\mathbf{k})[E_B^{\mathrm{hol}}(\mathbf{k})]^2 - [E_B^{\mathrm{hol}}(\mathbf{k})]^3}{[E_A^{\mathrm{hol}}(\mathbf{k}) - E_B^{\mathrm{hol}}(\mathbf{k})][E_B^{\mathrm{hol}}(\mathbf{k}) + E_B^{\mathrm{par}}(\mathbf{k})][E_B^{\mathrm{hol}}(\mathbf{k}) + E_A^{\mathrm{par}}(\mathbf{k})]}. \tag{14}$$

Here, the coefficients $D_0(\mathbf{k})$, $D_1(\mathbf{k})$, and $D_2(\mathbf{k})$ are functions of the zeroth-order excitation spectrum in t, and are given by

$$D_0(\mathbf{k}) = -[E_A^{\mathrm{par}}E_A^{\mathrm{hol}}(Un_B + E_B^{\mathrm{hol}}) + E_B^{\mathrm{par}}E_B^{\mathrm{hol}}(Un_A + E_A^{\mathrm{hol}})]/2 + \varepsilon(\mathbf{k})(Un_A + E_A^{\mathrm{hol}})(Un_B + E_B^{\mathrm{hol}}), \tag{15}$$

$$D_1(\mathbf{k}) = [(E_A^{\mathrm{hol}} - E_A^{\mathrm{par}})(Un_B + E_B^{\mathrm{hol}}) + (E_B^{\mathrm{hol}} - E_B^{\mathrm{par}})(Un_A + E_A^{\mathrm{hol}}) - E_A^{\mathrm{par}}E_A^{\mathrm{hol}} - E_B^{\mathrm{par}}E_B^{\mathrm{hol}}]/2 + \varepsilon(\mathbf{k})(Un_A + Un_B + E_A^{\mathrm{hol}} + E_B^{\mathrm{hol}}), \tag{16}$$

and

$$D_2(\mathbf{k}) = (Un_A + Un_B - E_A^{\mathrm{par}} - E_B^{\mathrm{par}})/2 + E_A^{\mathrm{hol}} + E_B^{\mathrm{hol}} + \varepsilon(\mathbf{k}). \tag{17}$$

Using the definition given above Eq. (2), the spectral function for the CDW phase can be easily obtained from Eq. (10), leading to $A_{\mathrm{CDW}}(\mathbf{k},\omega) = C_A^{\mathrm{par}}(\mathbf{k})\delta[\omega - E_A^{\mathrm{par}}(\mathbf{k})] + C_A^{\mathrm{hol}}(\mathbf{k})\delta[\omega + E_A^{\mathrm{hol}}(\mathbf{k})] + C_B^{\mathrm{par}}(\mathbf{k})\delta[\omega - E_B^{\mathrm{par}}(\mathbf{k})] + C_B^{\mathrm{hol}}(\mathbf{k})\delta[\omega + E_B^{\mathrm{hol}}(\mathbf{k})]$. Notice that this function satisfies the sum rule mentioned above Eq. (2), since the coefficients satisfy $C_A^{\mathrm{par}}(\mathbf{k}) + C_A^{\mathrm{hol}}(\mathbf{k}) + C_B^{\mathrm{par}}(\mathbf{k}) + C_B^{\mathrm{hol}}(\mathbf{k}) = 1$. The momentum distribution measures the spectral weight of the hole excitation spectrum as defined in Eq. (2), and for the CDW phase it is given by

$$n_{\mathrm{CDW}}(\mathbf{k}) = -C_A^{\mathrm{hol}}(\mathbf{k}) - C_B^{\mathrm{hol}}(\mathbf{k}). \tag{18}$$

This expression has a highly nontrivial dependence on t, and it has to be solved numerically together with the excitation spectrum. However, it can be analytically shown that the momentum distribution is flat and equals the average filling fraction $n_{\mathrm{CDW}}(\mathbf{k}) = (n_A + n_B)/2$ at zeroth order in t, corresponding to vanishing site-to-site correlations. To provide an independent check of the algebra (and to extend to finite dimensions), we next calculate $n(\mathbf{k})$ as a power-series expansion in the hopping t via the exact strong-coupling perturbation theory in d dimensions.

B. Strong-coupling Perturbation Theory

To determine the momentum distribution of the insulating phases, we need the wave function of the insulating state $|\Psi_{\mathrm{Ins}}\rangle$ as a function of t. We use the many-body version of Rayleigh-Schrödinger perturbation theory in the kinetic energy term [29] to perform the expansion (in powers of t) for $|\Psi_{\mathrm{Ins}}\rangle$ needed to carry out our analysis. A similar expansion for the ground-state energies was previously used to discuss the phase diagram of the on-site BH model [3,4], and it has recently been applied to the extended BH model [19]. For the on-site BH model, extrapolated results of these expansions showed an excellent agreement with recent quantum Monte Carlo simulations [5,6]. A high-order strong-coupling expansion for the ground-state energies has now been extended to all dimensions and fillings [30], and a high-order expansion for the wave function has also been used to describe the Mott phase in one-dimensional systems [31].

For our purpose, we first need the ground-state wavefunctions of the Mott and CDW phases when $t=0$. To zeroth order in t, the insulator (Mott or CDW) wave function can be written as

$$|\Psi_{\mathrm{Ins}}^{(0)}\rangle = \prod_{\ell \in A, \ell' \in B}^{M/2} \frac{(b_\ell^\dagger)^{n_A}}{\sqrt{n_A!}} \frac{(b_{\ell'}^\dagger)^{n_B}}{\sqrt{n_B!}} |0\rangle, \tag{19}$$

where M is the number of lattice sites, and $|0\rangle$ is the vacuum state (here, we remind that the lattice is divided equally into A and B sublattices). In principle, we can apply the perturbation theory on $|\Psi_{\mathrm{Ins}}^{(0)}\rangle$ to calculate $|\Psi_{\mathrm{Ins}}\rangle$ up to the desired order. However, since the number of intermediate states increases dramatically due to the presence of nearest-neighbor interactions, we perform this expansion only up to second order in t. The (unnormalized) wave function for the insulating state can then be written as

$$|\psi_{\mathrm{Ins}}\rangle = |\Psi_{\mathrm{Ins}}^{(0)}\rangle + \sum_{m \neq |\Psi_{\mathrm{Ins}}^{(0)}\rangle} \frac{T_{m0}}{E_{0m}} |\Psi_{\mathrm{Ins}}^{(0)}\rangle + \sum_{\{m',m\} \neq |\Psi_{\mathrm{Ins}}^{(0)}\rangle} \frac{T_{m'm}T_{m0}}{E_{0m'}E_{0m}} |\Psi_{\mathrm{Ins}}^{(0)}\rangle + O(t^3), \tag{20}$$

where $T_{m0} = -\Sigma_{S,S'}\Sigma_{\ell \in S, \ell' \in S'} t_{\ell\ell'} \langle m | b_\ell^\dagger b_{\ell'} | \Psi_{\mathrm{Ins}}^{(0)}\rangle$ is the hopping matrix element between the first-order intermediate state $|m\rangle$ and the zeroth-order state $|\Psi_{\mathrm{Ins}}^{(0)}\rangle$, and $T_{mm'}$ is between $|m\rangle$ and the second-order intermediate state $|m'\rangle$, and $E_{0m} = E_{\mathrm{Ins}}^{(0)} - E_m^{(0)}$. Here, the summation indices $\ell \in \{A,B\}$ and $\ell' \in \{A,B\}$ include the entire lattice, and S and S' label sublattices $\{A,B\}$. The $|m\rangle$ states are connected to $|\Psi_{\mathrm{Ins}}^{(0)}\rangle$ state with a single hopping, and similarly $|m'\rangle$ states are connected to $|m\rangle$ states with a single hopping. However, the $|m'\rangle$ state must be different from the $|\Psi_{\mathrm{Ins}}^{(0)}\rangle$ state.

To calculate the momentum distribution, we need the normalized wave function for the insulating state $|\Psi_{\mathrm{Ins}}\rangle$

$=|\psi_{\rm Ins}\rangle/\sqrt{\langle\psi_{\rm Ins}|\psi_{\rm Ins}\rangle}$, where the normalization up to second order in t is given by

$$\langle\psi_{\rm Ins}|\psi_{\rm Ins}\rangle = 1 + \frac{n_A(n_B+1)Mzt^2/2}{[U(n_A-n_B-1)+V(zn_B-zn_A+1)]^2} + \frac{n_B(n_A+1)Mzt^2/2}{[U(n_B-n_A-1)+V(zn_A-zn_B+1)]^2} + O(t^4). \tag{21}$$

Here, $z=2d$ is the lattice coordination number. Since $\langle m|\Psi_{\rm Ins}^{(0)}\rangle=\langle m''|\Psi_{\rm Ins}^{(0)}\rangle=\langle m'|m\rangle=0$, the first- and third-order terms in t vanish in the normalization. In general, all odd-order terms in t vanish.

A lengthy but straightforward calculation leads to the momentum distribution, defined in Eq. (3), up to second order in t as

$$\begin{aligned} n_{\rm Ins}(\mathbf{k}) = {} & \frac{n_A+n_B}{2} + \left[\frac{n_A(n_B+1)}{U(n_A-n_B-1)+V(zn_B-zn_A+1)} + \frac{n_B(n_A+1)}{U(n_B-n_A-1)+V(zn_A-zn_B+1)}\right]\varepsilon(\mathbf{k}) \\ & + \left\{\frac{n_A(n_B+1)}{2[U(n_A-n_B-1)+V(zn_B-zn_A+1)]^2} + \frac{n_B(n_A+1)}{2[U(n_B-n_A-1)+V(zn_A-zn_B+1)]^2} \right. \\ & \left. - \frac{n_A(n_B+1)}{U[U(n_A-n_B-1)+V(zn_B-zn_A+1)]} - \frac{n_B(n_A+1)}{U[U(n_B-n_A-1)+V(zn_A-zn_B+1)]}\right\} \\ & \times(n_A+n_B+1)[\varepsilon^2(\mathbf{k})-2dt^2] + O(t^3). \end{aligned} \tag{22}$$

In the definition of the momentum distribution, the summation indices $\ell\in\{A,B\}$ and $\ell'\in\{A,B\}$ include the entire lattice. Here, $\varepsilon(\mathbf{k})=-(2/M)\Sigma_{\ell\in S,\ell'\in S'}t_{\ell\ell'}e^{i\mathbf{k}\cdot(\mathbf{R}_\ell-\mathbf{R}_{\ell'})}$ is the Fourier transform of the hopping matrix $t_{\ell,\ell'}$ (energy dispersion), and $\varepsilon^2(\mathbf{k})-2dt^2=(2/M)\Sigma_{\{\ell,\ell''\}\in S,\ell'\in S'}t_{\ell\ell'}t_{\ell'\ell''}e^{i\mathbf{k}\cdot(\mathbf{R}_\ell-\mathbf{R}_{\ell''})}$, where the summation indices $\{\ell,\ell''\}\in A$ (or B) and $\ell'\in B$ (or A) include only one sublattice. Since there are $M/2$ lattice sites in one sublattice, a factor of 2 appears in these expressions. To zeroth order in t, Eq. (22) shows that $n_{\rm Ins}(\mathbf{k})$ is flat and equals the average filling fraction $(n_A+n_B)/2$. However, it develops a peak around $\mathbf{k}=0$ and a minimum around $\mathbf{k}=\boldsymbol{\pi}$ at first order in t. These general observations are consistent with the RPA results shown in Eqs. (9) and (18).

Equation (22) is valid for the insulating phases of all d-dimensional hypercubic lattices. For instance, when $n_A=n_B=n_0$, Eq. (22) reduces to the momentum distribution for the Mott phase, i.e.,

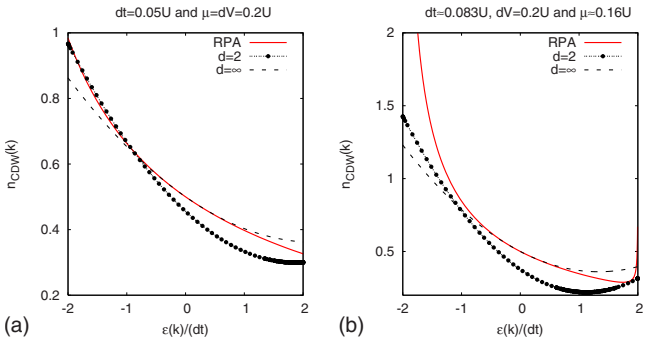

FIG. 2. (Color online) Momentum distribution $n_{\rm CDW}(\mathbf{k})$ versus $\varepsilon(\mathbf{k})/(dt)$ for a $(d=2)$- and $(d\to\infty)$-dimensional hypercubic lattices. Panel (a) has the nearest-neighbor boson-repulsion satisfying $dV=0.2U$, the hopping satisfying $dt=0.05U$, and the chemical potential set by $\mu=0.2U$ corresponding approximately to the center of the first CDW lobe, and panel (b) has $dV=0.2U$, $dt\approx0.083U$, and $\mu\approx0.16$ corresponding approximately to the tip of the first CDW lobe. The solid (red) lines correspond to the RPA, and the dashed and circled lines to the second-order strong-coupling perturbation theory for different dimensions. The peak occurs at the zone corner only when the hopping is close to the tip of the CDW lobe.

$$n_{\rm Mott}(\mathbf{k}) = n_0 - 2n_0(n_0+1)\frac{\varepsilon(\mathbf{k})}{U-V} + n_0(n_0+1)(2n_0+1) \times[\varepsilon^2(\mathbf{k})-2dt^2]\frac{3U-2V}{U(U-V)^2} + O(t^3). \tag{23}$$

This expression recovers the known result for the on-site BH model when $V=0$ [32,33]. In addition, in the $d\to\infty$ limit, we checked that Eqs. (22) and (23) agree with the RPA solutions (which are exact in this limit) given in Eqs. (18) and (9) when the latter are expanded out to second order in t, providing an independent check of the algebra. One must note that the terms $2V$ and V that appear in the numerator and denominator of Eq. (23) vanish in the limit when $d\to\infty$ because $V\propto 1/d$. Next, we compare the RPA results with those of the strong-coupling perturbation theory.

C. Numerical Results

Since the momentum distribution of the CDW phase given in Eq. (18) has a highly nontrivial dependence on t, it has to be solved numerically together with the excitation spectrum. Next, we set $dV=0.2U$ and solve this equation for the first CDW lobe. For this parameter, we remind that the $t=0$ chemical potential width of all Mott and CDW lobes are U and $0.4U$, respectively, and that the ground state alternates between the CDW and Mott phases as a function of μ. For instance, the ground state is a vacuum $(n_0=0)$ for $\mu\le0$; it is a CDW with $(n_A=1,\ n_B=0)$ for $0\le\mu\le0.4U$; it is a Mott insulator with $(n_0=1)$ for $0.4U\le\mu\le1.4U$; it is a CDW with $(n_A=2,\ n_B=1)$ for $1.4U\le\mu\le1.8U$; it is a Mott insulator with $(n_0=2)$ for $1.8U\le\mu\le2.8U$.

In Fig. 2, the results of the RPA calculation given in Eq. (18) are compared to those of the second-order strong-coupling perturbation theory given in Eq. (22) for a $(d=2)$- and $(d\to\infty)$-dimensional hypercubic lattices. In this figure,

we show the momentum distribution $n_{\mathrm{CDW}}(\mathbf{k})$ as a function of $\varepsilon(\mathbf{k})/(dt)$ for two sets of parameters. In Fig. 2(a), we choose $dt=0.05U$ and $\mu=0.2U$, which approximately corresponds to the center of the first CDW lobe. For this parameter set, deep inside the CDW lobe, the momentum distribution has a peak at $\varepsilon(\mathbf{k})=-2dt$ corresponding to the $\mathbf{k}=0$ point, and it has a minimum at $\varepsilon(\mathbf{k})=2dt$ corresponding to the $\mathbf{k}=(\pi,\pi,\ldots)$ point. This is very similar to what happens in the Mott phase. However, in Fig. 2(b), we choose $dt \approx 0.083U$ and $\mu \approx 0.16U$, which approximately corresponds to the tip of the first CDW lobe. For this parameter set, close to the CDW-supersolid phase transition, the momentum distribution has two peaks: a large peak at $\varepsilon(\mathbf{k})=-2dt$ corresponding to the $\mathbf{k}=0$ point, and a smaller one at $\varepsilon(\mathbf{k})=2dt$ corresponding to the $\mathbf{k}=(\pi,\pi,\ldots)$ point. The second peak is unique to the CDW phase and it does not occur in a Mott phase. Notice that both the RPA and second-order strong-coupling expansion give qualitatively similar results (although the peak is much sharper and has lower weight in the exact solution).

One might have expected to always see the peak in the momentum distribution at the $\mathbf{k}=(\pi,\pi,\ldots)$ point due to the reduced periodicity of the CDW order. But because the momentum distribution involves four terms corresponding the *AA*, *AB*, *BA*, and *BB* sublattice combinations, only the first and last terms are periodic in the reduced Brillouin zone. Deep inside the CDW lobe, the presence of a large gap in the one-particle excitation spectrum produces an exponential decay of the one-particle correlations, which suppresses this peak in the momentum distribution as can be seen in Fig. 2(a) (this point has already been discussed in Ref. [34]). This essentially occurs because there is a cancellation of the peak that arises from the *AA* and *BB* contributions with the results from the *AB* and *BA* pieces, similar to what happens in the Mott phase. However, close to the tip of the CDW lobe, the peak emerges in the exact solution of the RPA as shown in Fig. 2(b).

As a further check of the accuracy of our second-order strong-coupling expansion, in Fig. 3, we compare the $d=2$ and $d\to\infty$ limits of Eq. (22) to the RPA method given in Eq. (18), which corresponds to the exact solution in the latter limit. In this figure, we show $n_{\mathrm{CDW}}(\mathbf{k}=0)$ and $n_{\mathrm{CDW}}(\mathbf{k}=\boldsymbol{\pi})$ as a function of dt/U when $\mu=0.2U$. In $d=2$ dimensions, the RPA and second-order strong-coupling expansion gives qualitatively similar results for small values of dt/U, i.e., deep inside the CDW lobe. However, in the $d\to\infty$ limit, the results of the RPA and the second-order strong-coupling expansion match exactly for small values of dt/U (as they must). Close to the tip of the CDW lobe, the RPA and strong-coupling results differ substantially from each other signaling the breakdown of the second-order expansion. However, both theories show that $n_{\mathrm{CDW}}(0)$ is an increasing function of dt/U as one may expect. This is because the range of μ about which the ground state is a CDW decreases as dt/U increases from zero, and the CDW phase becomes a supersolid at a critical value of $dt_c \sim 0.08U$. Beyond this point, $n(0)$ diverges due to the appearance of a condensate, corresponding to the macroscopic occupation of the $\mathbf{k}=0$ state.

Note that we do not attempt to perform a scaling analysis of the momentum distribution for the CDW phase. The reasons why are twofold. First, we only have the series through second order, which probably is too short to be able to properly fit to a phenomenological scaling form, and second, we cannot extract the analytic scaling form from the RPA calculation anymore, so guessing an appropriate phenomenological form has less guidance than for the Mott phase. A scaled theory would be expected to be accurate for all values of t within the insulating phases, as has been recently shown for the Mott phase of the on-site BH model [32].

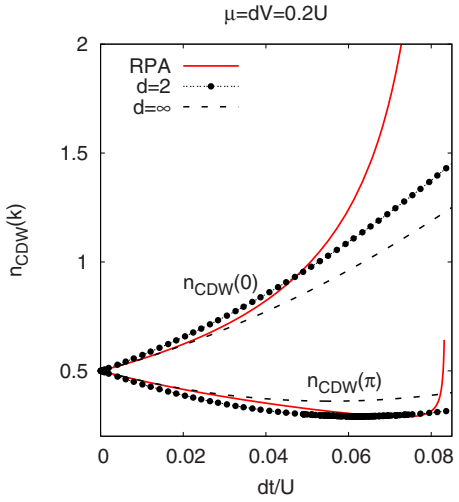

FIG. 3. (Color online) Momentum distributions at specific momentum points $n_{\mathrm{CDW}}(\mathbf{k}=0)$ and $n_{\mathrm{CDW}}(\mathbf{k}=\boldsymbol{\pi})$ versus dt/U for $(d=2)$- and $(d\to\infty)$-dimensional hypercubic lattices. The chemical potential $\mu=dV$ corresponds to the first CDW lobe, and the nearest-neighbor repulsion is set to $dV=0.2U$. The solid line corresponds to the RPA and the dashed and circled lines to the second-order strong-coupling perturbation theory for different dimensions.

IV. CONCLUSIONS

We developed two methods to calculate the momentum distribution of the insulating (Mott and charge-density-wave) phases of the extended Bose-Hubbard model with on-site and nearest-neighbor boson-boson repulsions on d-dimensional hypercubic lattices. First, we analyzed the momentum distribution within the random-phase approximation, which corresponds to the exact solution for the infinite-dimensional limit. Then, we used the many-body version of the Rayleigh-Schrödinger perturbation theory in the kinetic energy term, and derived the wave function for the insulating phases as a power series in the hopping t, to calculate the momentum distribution via the strong-coupling perturbation theory. A similar strong-coupling expansion for the ground-state energies was previously used to discuss the phase diagram of the on-site BH model [3,4], and it has recently been applied to the extended BH model [19].

The agreement between the second-order strong-coupling expansion and that of RPA method is only qualitative in low-dimensional systems. This is not surprising since the fluctuations are not fully taken into account in the RPA method. However, we showed that our strong-coupling expansion matches exactly the RPA result (as it must) in the infinite-

dimensional limit when the latter is expanded out in t to the same order. We believe some of these results could potentially be tested with ultracold dipolar Bose gases loaded into optical lattices [35]. This work can be extended in several ways if desired. For instance, one could calculate the momentum distribution up to third order in t, and develop a scaling theory with the help of the RPA results (or a good phenomenological guess for the scaling form of the momentum distribution). The scaled theory is expected to be accurate for all values of t within the insulating phases, as has been recently shown for the Mott phase of the on-site BH model [32].

ACKNOWLEDGMENTS

We would like to acknowledge useful discussions with H. R. Krishnamurthy and M. Rigol. J.K.F. acknowledges support under the USARO Grant No. W911NF0710576 with funds from the DARPA OLE Program.

[1] D. Jaksch, C. Bruder, J. I. Cirac, C. W. Gardiner, and P. Zoller, Phys. Rev. Lett. **81**, 3108 (1998).
[2] M. P. A. Fisher, P. B. Weichman, G. Grinstein, and D. S. Fisher, Phys. Rev. B **40**, 546 (1989).
[3] J. K. Freericks and H. Monien, EPL **26**, 545 (1994).
[4] J. K. Freericks and H. Monien, Phys. Rev. B **53**, 2691 (1996).
[5] B. Capogrosso-Sansone, N. V. Prokof'ev, and B. V. Svistunov, Phys. Rev. B **75**, 134302 (2007).
[6] B. Capogrosso-Sansone, S. G. Söyler, N. Prokof'ev, and B. Svistunov, Phys. Rev. A **77**, 015602 (2008).
[7] D. van Oosten, P. van der Straten, and H. T. C. Stoof, Phys. Rev. A **63**, 053601 (2001).
[8] M. Greiner, O. Mandel, T. Esslinger, T. W. Hänsch, and I. Bloch, Nature (London) **415**, 39 (2002).
[9] I. B. Spielman, W. D. Phillips, and J. V. Porto, Phys. Rev. Lett. **98**, 080404 (2007).
[10] I. B. Spielman, W. D. Phillips, and J. V. Porto, Phys. Rev. Lett. **100**, 120402 (2008).
[11] F. Gerbier, S. Trotzky, S. Fölling, U. Schnorrberger, J. D. Thompson, A. Widera, I. Bloch, L. Pollet, M. Troyer, B. Capogrosso-Sansone, N. V. Prokof'ev, and B. V. Svistunov, Phys. Rev. Lett. **101**, 155303 (2008).
[12] K. Góral, L. Santos, and M. Lewenstein, Phys. Rev. Lett. **88**, 170406 (2002).
[13] C. Bruder, Rosario Fazio, and Gerd Schön, Phys. Rev. B **47**, 342 (1993).
[14] Parhat Niyaz, R. T. Scalettar, C. Y. Fong, and G. G. Batrouni, Phys. Rev. B **50**, 362 (1994).
[15] Anne van Otterlo, Karl-Heinz Wagenblast, Reinhard Baltin, C. Bruder, Rosario Fazio, and Gerd Schön, Phys. Rev. B **52**, 16176 (1995).
[16] T. D. Kühner, S. R. White, and H. Monien, Phys. Rev. B **61**, 12474 (2000).
[17] D. L. Kovrizhin, G. Venketeswara Pai, and S. Sinha, EPL **72**, 162 (2005).
[18] C. Trefzger, C. Menotti, and M. Lewenstein, Phys. Rev. A **78**, 043604 (2008).
[19] M. Iskin and J. K. Freericks, Phys. Rev. A **79**, 053634 (2009).
[20] A. J. Leggett, Phys. Rev. Lett. **25**, 1543 (1970).
[21] S. Ospelkaus, A. Pe'er, K.-K. Ni, J. J. Zirbel, B. Neyenhuis, S. Kotochigova, P. S. Julienne, J. Ye, and D. S. Jin, Nat. Phys. **4**, 622 (2008).
[22] K.-K. Ni, S. Ospelkaus, M. H. G. de Miranda, A. Pe'er, B. Neyenhuis, J. J. Zirbel, S. Kotochigova, P. S. Julienne, D. S. Jin, and J. Ye, Science **322**, 231 (2008).
[23] S. Haley and P. Erdös, Phys. Rev. B **5**, 1106 (1972).
[24] K. Sheshadri, H. R. Krishnamutry, R. Pandit, and T. V. Ramakrishnan, EPL **22**, 257 (1993).
[25] K. Sengupta and N. Dupuis, Phys. Rev. A **71**, 033629 (2005).
[26] C. Menotti and N. Trivedi, Phys. Rev. B **77**, 235120 (2008).
[27] S. Konabe, T. Nikuni, and M. Nakamura, Phys. Rev. A **73**, 033621 (2006).
[28] Y. Ohashi, M. Kitaura, and H. Matsumoto, Phys. Rev. A **73**, 033617 (2006).
[29] L. D. Landau and L. M. Lifshitz, *Quantum Mechanics* (Butterworth-Heinemann, Burlington, MA, 1981).
[30] N. Teichmann, D. Hinrichs, M. Holthaus, and A. Eckardt, Phys. Rev. B **79**, 100503(R) (2009).
[31] B. Damski and J. Zakrzewski, Phys. Rev. A **74**, 043609 (2006).
[32] J. K. Freericks, H. R. Krishnamurthy, Yasuyuki Kato, Naoki Kawashima, and Nandini Trivedi, Phys. Rev. A **79**, 053631 (2009).
[33] A. Hoffmann and A. Pelster, Phys. Rev. A **79**, 053623 (2009). These authors have applied a similar second-order strong-coupling expansion to describe the momentum distribution of the Mott phase of the on-site BH model in three dimensions. Their coefficient for the second-order term is missing an overall factor of 3.
[34] V. G. Rousseau, D. P. Arovas, M. Rigol, F. Hébert, G. G. Batrouni, and R. T. Scalettar, Phys. Rev. B **73**, 174516 (2006). A similar peak at $\mathbf{k}=(\pi,\pi,\ldots)$ emerges for the same reason in the presence of a superlattice potential as shown in Fig. 9.
[35] In the case of dipolar Bose gases, we would like to remark that cutting the long-range part of the interaction is questionable only if one wants to illustrate the devil's staircase, which requires infinitesimal t, or very very large U, so large that the use of the single-band model picture becomes questionable. Also, it is hard to see how one can image the phase if it is present in a very small range of μ, which is the case for high period phases. On the other hand, as explicitly shown for the Mott phases, the nearest-neighbor interaction does essentially nothing to change the mean-field phase boundary or the RPA momentum distribution. We expect the same to be true for the CDW phase, such that inclusion of the longer-ranged interactions will not modify the phase boundary or the RPA momentum distribution much.